JOURNAL OF CATALYSIS 139, 277–288 (1993)

Selective Catalytic Reduction of NO with NH_3 on SO_4^{-2}/TiO_2 Superacid Catalyst

J. P. CHEN AND R. T. YANG[1]

Department of Chemical Engineering, State University of New York at Buffalo, Buffalo, New York 14260

Received March 20, 1992; revised August 4, 1992

SO_4^{-2}/TiO_2 superacid is studied for selective catalytic reduction (SCR) of NO with NH_3. Since SO_4^{-2}/TiO_2 is formed on TiO_2 under SCR reaction conditions when SO_2 is present, the results also elucidate the role of TiO_2 support (and SO_2) in the SCR reaction. SO_4^{-2}/TiO_2 exhibits a considerable activity, exceeding that of V_2O_5/TiO_2 at temperatures above 400°C, and reaches a peak activity at 500–525°C. TGA, XPS, and IR analyses of the catalyst indicate that SO_4^{-2} ions are formed on TiO_2, and the structure of the TiO_2 surface sulfate under the SCR reaction conditions is bridged bidentate, $Ti_2SO_3(OH)$. XPS and chemisorption measurements along with SCR kinetic results indicate that the reaction takes place by an Eley–Rideal mechanism, on Brønsted-acid sites on SO_4^{-2}/TiO_2 surface. At 400°C, about 70% of the SO_4^{-2} ions are occupied by ammonia, and about a half of the chemisorbed ammonia is active for reaction with NO.

INTRODUCTION

The commercial catalysts for selective catalytic reduction (SCR) of NO with NH_3 are TiO_2 supported V_2O_5-based catalysts (*1*). These catalysts are highly active in the reaction temperature range 250–350°C. Further increase in reaction temperature results in oxidation of NH_3, which not only decreases the catalytic activity but also produces NO_x (*2*). It is thus of interest to have an active catalyst for temperatures higher than 350°C.

Our earlier results (*2–4*) showed that the addition of SO_2 in the reactants increases the SCR activity for the V_2O_5/TiO_2 catalyst. A possible reason for the promotion by SO_2 is the formation of surface SO_4^{-2} which would change the catalyst surface acidity. The acid strengths for the sulfated metal oxides are high. It has been reported that for SO_4^{-2}/TiO_2 (*5*) and SO_4^{-2}/ZrO_2 (*6, 7*), the Hammett acidity, $H_0 \leq -14.52$ and $H_0 \geq -14.52$, respectively, as compared with that of H_2SO_4, $H_0 \leq -12$ (*8, 9*). Hence, these solids are referred to as solid superacids (*10–12*). The sulfate-promoted oxides, such as SO_4^{-2}/TiO_2, SO_4^{-2}/ZrO_2, and SO_4^{-2}/Fe_2O_3, are highly active for reactions such as isomerization of hydrocarbons and dehydration of alcohols.

Research on superacids for homogeneous catalysis has been active during the last 3 decades, mostly for the purpose of organic synthesis (*13*). More recently, increasing applications for solid superacids are being found in heterogeneous catalysis, for a wide variety of applications such as hydrocarbon isomerization, cracking, hydrocracking, dehydration, and alkylation. However, the solid superacids have not been used for selective catalytic reduction of NO with NH_3. Thus, the first intent of this work was to study the activity and mechanism of solid superacid for the SCR reaction. We report first results on sulfated titania alone (without vanadia), SO_4^{-2}/TiO_2, as a catalyst for NO reduction with NH_3. The results demonstrate that SO_4^{-2}/TiO_2 catalyst is very active for SCR at temperatures higher than 400°C.

Since it is known that both TiO_2 and V_2O_5 are present on the surfaces of V_2O_5/TiO_2 catalysts even with V_2O_5 amounts well

[1] To whom correspondence should be addressed.

0021-9517/93 $5.00

above monolayer (*14–16*), the second intent of this work was to elucidate the role of TiO_2 in SCR under practical conditions where surface sulfate is formed by reacting TiO_2 with SO_2 and O_2.

EXPERIMENTAL

Catalyst Preparation

Pelleted titanium dioxide was prepared by densification of TiO_2 powder (P25, Degussa) (*2, 3, 17*). One gram of titania powder was thoroughly mixed with 1.75 g of distilled water. The resulting paste was air dried in an oven at 60°C for 24 h and at 120°C for 72 h before crushing and sieving to collect the 20–32 mesh fraction. The collected fraction was subsequently calcined at 600°C first in air for 1 h, then in helium for 6 h.

Sulfation of the TiO_2 surface was achieved by reacting TiO_2 with SO_2 and O_2 under typical SCR reaction conditions. Two types of sulfation conditions were used: (1) 400°C, 500 ppm SO_2 and 2% O_2 in N_2; (2) same as above with the addition of 1000 ppm each of NH_3 and NO, and 8% H_2O (i.e., SCR reaction conditions). The resulting catalysts exhibited the same behaviors and were denoted as SO_4^{-2}/TiO_2.

The 5% V_2O_5/TiO_2 sample was prepared by incipient wetness impregnation with NH_4VO_3 followed by calcination. Details of the procedure and catalyst characterization are given elsewhere (*3*).

Catalytic Activity Measurement

The reactor was made of quartz that was heated by coiled Nichrome wire. The reactor temperature was controlled by a programmable temperature controller (Omega CN-2010). The catalyst was supported on a fritted quartz support.

The simulated flue gas was made by blending the gaseous reactants. The flow rates of the reactants were controlled by two sets of flow meters. Rotameters were used to control flows with high flow rates (i.e., N_2, NH_3/N_2, NO/N_2); mass flow meters were used for gases with low flow rates (SO_2 and O_2). The premixed gases (0.8% NO in N_2 and 0.8% NH_3 in N_2) were supplied by Linde Division. The 8% water vapor was generated by passing nitrogen through a heated gas-washing bottle containing distilled water. The tubings were wrapped with heating tapes to prevent the deposition of ammonium sulfate. NO concentration was continually monitored by a chemiluminescent NO/NO_x analyzer (Thermo Electron Corporation, Model 10). A quadruple mass spectrometer (UTI-100C) was connected to the reactor for analyzing reaction products. To avoid any error caused by oxidation of ammonia in the converter of the NO/NO_x analyzer, an ammonia trap (containing phosphoric acid solution) was installed before the sample inlet.

The rate constants were calculated based on assuming plug flow. The catalyst activity was expressed by the first order rate constant with respect to NO,

$$k = -\frac{F_0 \ln(1 - X)}{[NO]_0 W},$$

where W is the weight of the catalyst, F_0 is the inlet molar flowrate of NO, $[NO]_0$ is the inlet molar concentration, and X is NO conversion. In our previous work (*2–4, 51, 52*), the rate constants were calculated without considering the temperature effects on the reactant concentration, $[NO]_0$, which resulted in an error in the k value by a factor of 1.5–2.4, depending on the reaction temperature. (However, all conclusions remain correct.) In this work, both F_0 and $[NO]_0$ were calculated at the reaction temperature.

Strictly, the flow pattern in the reactor was not ideal plug flow and the reaction order was not exactly first order with respect to NO. However, most of the kinetics study results showed that SCR reaction is first order with respect to NO on a wide variety of metal oxides (*1, 3, 27, 31, 54, 55*). Nam *et al.*(*53*) developed a two-parameter model to include both SCR and NH_3 oxidation reactions, which fitted a wide range of reaction temperatures (from 250 to 500°C). At temperatures below the peak temperature of the NO SCR reaction, the model reduced to

pseudo-first-order behavior. This was commonly observed for the SCR reaction (*1, 3, 27, 31, 54, 55*). Since most of the activity measurements undertaken in this study were below or near the peak temperatures, all of the rate constant calculations were based on the assumption of plug flow and first order with respect to NO. Moreover, the rate constants were used for comparison, on the same basis, for the relative activities of different catalysts.

TGA and BET Measurements

Thermo-gravimetric analysis (TGA) experiments were performed in a Cahn 1000 electrobalance system (Cahn/Ventron Co.). The heating rate was 2°C/min. The BET surface area was measured with a Quantasorb using N_2 at 77k.

XPS Analysis

X-ray photoelectron spectra were measured with a Perkin–Elmer PHI 5100 XPS Spectrometer, using Mgkα as the radiation source. After SCR reaction or sulfation, the catalysts were cooled to room temperature in the reaction atmosphere and were purged in N_2 for 1 h. The catalyst pellets were then crushed and pressed into the sample holder on a double-side glue tape. The samples were degassed at ca. 10^{-6} Torr in the preparation chamber. The residual vacuum was maintained at 4×10^{-9} Torr during analysis. Charging effects were calibrated by C(1*s*) line at 284.5 eV.

FT-IR Spectra

FT-IR spectra were measured with an Alpha Centauri FT-IR spectrometer (Mattson Instruments, Inc.) at the ambient temperature. The catalysts were subjected to reaction for 7 days followed by cooling in the reactant atmosphere and purge in N_2 for 1 h. The samples were then ground, mixed, and pelletized with potassium bromide. The ratio of sample to potassium bromide was 5 : 100. The spectrum was obtained as the ratio of sample to TiO_2.

Ammonia Oxidation and Chemisorption

Ammonia oxidation experiments were carried out by passing 1000 ppm ammonia in nitrogen and other gases (i.e., 2% O_2, 8% H_2O, and balance N_2) through the catalyst bed. The chemiluminescent NO_x analyzer was used to measure the concentration of NO_x produced by oxidation.

The amount of ammonia chemisorption at 400°C was measured by using the same reactor system. The influent to the packed bed (with 0.5 ml catalyst) was 1000 ppm NH_3 in nitrogen, and the effluent was directly fed to the chemiluminescent analyzer. A high-temperature converter in the analyzer converted ammonia by the reaction $NH_3 + O_2 \rightarrow NO_x + H_2O$. Thus the concentration of ammonia could be measured. The chemisorbed amount was the difference between the total amounts of NO, integrated over time, contained in the influent and effluent.

RESULTS AND DISCUSSION

SCR Activity and Rate Constant Measurements

The SCR activities were measured by temperature-programmed reaction (TPR) and/or under steady-state conditions. To avoid effects of SO_2, no SO_2 was introduced in these reactions. The reaction products on SO_4^{-2}/TiO_2 were analyzed by mass spectrometry, with particular attention to N_2O. Fragmentation of NO was accounted for in the analyses. The mass spectrometry results showed no detectable (of the order of ppm detection limit) N_2O in the products under the reaction conditions covered in this study. Similar results with respect to product selectivity were reported for the V_2O_5-based catalysts (*49*).

The TPR results are shown in Fig. 1 for TiO_2 and SO_4^{-2}/TiO_2. TiO_2 is inactive for SCR at temperatures below 350°C. It does, however, exhibit some activity at temperatures above 400°C. After sulfation of the surface of TiO_2, the SCR activity increased substantially. (The characterization of the SO_4^{-2}/TiO_2 surface will be given shortly.)

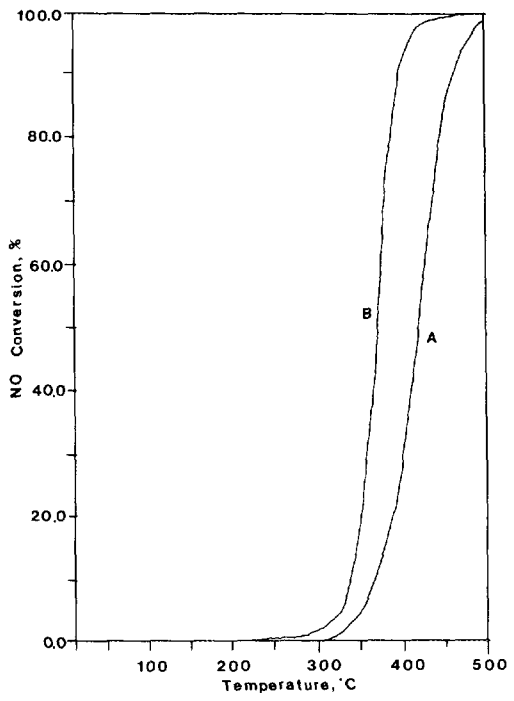

FIG. 1. Temperature-programmed reaction of NO with NH_3 on TiO_2 (A) and SO_4^{-2}/TiO_2 (B). Reaction conditions: NO = NH_3 = 1000 ppm, O_2 = 2%, H_2O = 8%, N_2 = balance, GHSV = 15,000 h^{-1}, heating rate = 10°C, catalyst weight = 1.60 g, catalyst volume = 2 ml.

The steady-state SCR activity results are shown in Table 1. Here three catalysts are compared: TiO_2, SO_4^{-2}/TiO_2, and 5% V_2O_5/TiO_2. It is obvious that while the V_2O_5/TiO_2 catalyst is superior at temperatures below 400°C, the SO_4^{-2}/TiO_2 becomes increasingly more active as the temperature is increased beyond 400°C. The SO_4^{-2}/TiO_2 activity continues to increase with temperature (Fig. 1), whereas the activity of V_2O_5/TiO_2 catalyst declines precipitously (*2*).

As discussed by Nam *et al.* (*53*) and in our work (*2*), the high-temperature declination of NO SCR activity is caused by the oxidation of NH_3. The NH_3 oxidation activities of the three catalysts are compared in Table 2. The results show that V_2O_5/TiO_2 has the highest NH_3 oxidation activity

TABLE 1

NO Conversion on TiO_2, SO_4^{-2}/TiO_2, and V_2O_5/TiO_2

Temperature (°C)	NO conversion (%)		
	TiO_2	SO_4^{-2}/TiO_2	5% V_2O_5/TiO_2
350	4.0	15.0	99.9
400	15.0	96.0	99.9
410	32.0	98.3	86.2
425	46.5	99.7	75.0

Note. Reaction conditions: NO = NH_3 = 1000 ppm, O_2 = 2%, N_2 = balance, GHSV = 15,000 h^{-1}, catalyst weight = 1.60 g, reactant gas flow rate = 500 ml STP/min.

whereas the SO_4^{-2}/TiO_2 catalyst has the lowest activity.

At temperatures above 400°C, the reaction conditions listed in Table 1 lead to NO conversions too high for accurate determination for the rate constant. Thus the space velocity was reduced for measuring the SCR activities at higher temperatures, shown in Table 3. The SCR activity for SO_4^{-2}/TiO_2 continues to increase with temperature until peaking in the range 500–525°C, followed by a slow decline. A catalyst stability run was made at 550°C; no decline in activity was shown after 24 h. The high activities in this temperature range are promising for high-temperature applications.

On the TiO_2 surfaces, both Lewis acid sites (*18*) and Brønsted-acid sites (*19, 20*)

TABLE 2

Ammonia Oxidation on Different Catalysts

Temperature (°C)	NO produced (ppm)		
	TiO_2	SO_4^{-2}/TiO_2	5% V_2O_5/TiO_2
350	2	1	2
400	6	3	12
410	8	4	18
425	14	6	35

Note. Reaction conditions: NH_3 = 1000 ppm, O_2 = 2%, N_2 balance, total gas flow rate = 500 ml STP/min, catalyst weight = 1.0 g.

TABLE 3

High-Temperature SCR Activities on SO_4^{-2}/TiO_2

Temperature (°C)	NO conv. (%)	k($cm^3/g/s$)
400	63.0	16.6
425	90.0	38.4
475	93.0	44.3
500	93.7	46.1
525	93.5	45.6
550	91.0	40.1
575	83.0	29.5

Note. Reaction conditions: NO = NH_3 = 1000 ppm, O_2 = 2%, SO_2 = 500 ppm, N_2 = balance, catalyst weight = 0.5 g, total gas flow rate = 500 ml STP/min.

exist depending on its preparation and pretreatment. Generally, the acid sites are Brønsted type when calcined at low temperatures and Lewis type at high temperatures (*19, 20*). The introduction of sulfate ions on the TiO_2 surface can generate superacidity (*21*) as well as Brønsted acidity (*50*). The direct relationship between the Brønsted acidity and the SCR activity (and evidence for the relationship reported in the literature) has been discussed (*2–4, 54*). The increased SCR activity for the SO_4^{-2}/TiO_2 catalyst shown in Fig. 1 and Tables 1 and 3 is clear evidence of the generation of superacidity. The characterization of the surface SO_4^{-2} ions is given in the subseqent sections.

The effects of water vapor on the SO_4^{-2}/TiO_2 catalyst is shown in Table 4, for 400 and 410°C. When water vapor was switched off from the reactant mixture, the NO conversion increased rapidly, and the water effect was reversible. A possible interpretation of this result is that water competes with NH_3 for chemisorption, which is a necessary step in the reaction as to be discussed later.

TABLE 4

SCR Activities of SO_4^{-2}/TiO_2

Temperature (°C)	Water vapor	NO conversion (%)	Rate constant ($cm^3/g/s$)
400	With	80.0	16.76
	Without	92.5	26.98
410	With	94.5	30.21
	Without	97.9	40.24

Note. Reaction conditions: NO = NH_3 = 1000 ppm, O_2 = 2%, H_2O = 8% GHSV = 30,000 h^{-1}, catalyst weight = 0.80 g, catalyst volume = 1 ml, reactant gas flow rate = 500 ml STP/min.

Sulfation of TiO_2 during SCR Reaction

A variety of techniques has been reported in the literature for introducing SO_4^{-2} ions to the surfaces of metal oxides. Among them are impregnation with H_2SO_4 or $(NH_4)_2SO_4$ solution (*23–25*), reacting with SO_3, SO_2 or H_2S followed by oxidation (*22, 25*).

Two types of treatment for TiO_2 were used in this study: reacting with 500 ppm SO_2 and 2% O_2 in N_2 at 400°C, or with the further addition of 1000 ppm each of NH_3 and NO and 8% H_2O (i.e., under typical SCR conditions). The SCR activities of catalysts from these two treatments were identical.

Transient SCR results, shown in Fig. 2, are used to illustrate the relationship between SCR activity and sulfation. The NO conversion was 14% before SO_2 injection into the SCR reactants. Figure 2 shows the responses in NO conversion upon injection of different SO_2 concentrations. At low SO_2 concentration and with short sulfation time, the rate constants contributed from uncover. TiO_2 could not be ignored. As the sulfation proceed, the contribution from TiO_2 become negligible. In order to understand the relationship between SO_2 concentration (or extent of sulfation) and the NO SCR activity, the transient results are presented in Table 5, in terms of SCR rate constants for the first 30 min. The rate constant was approximately proportional to SO_2 concentration. This result indicates that the rate of sulfation was dependent on the concentration of SO_2 and that the SCR activity was directly related to the extent of sulfation. The sulfation was completed in about 90 min. After the sulfation was completed,

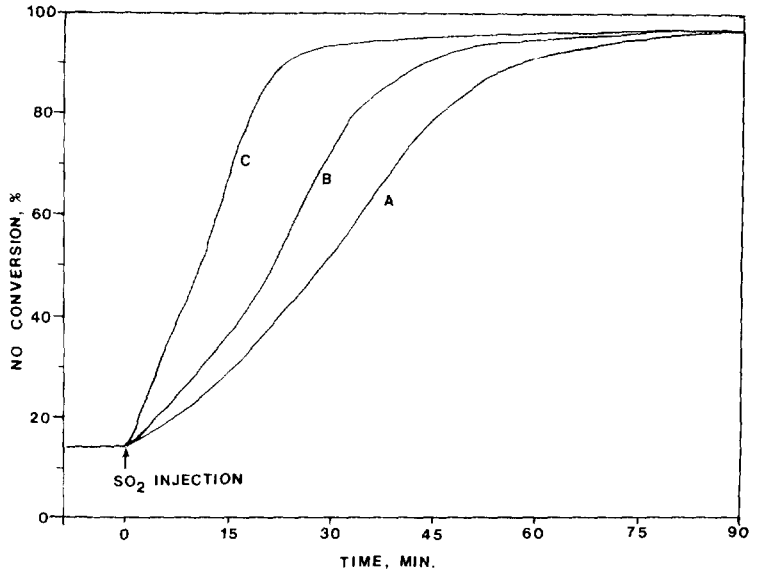

FIG. 2. Dependence of NO conversion on TiO_2 surface sulfation with different SO_2 concentration. (A) SO_2 = 250 ppm; (B) SO_2 = 500 ppm; (C) SO_2 = 1000 ppm. Other reaction conditions: NO = NH_3 = 1000 ppm, O_2 = 2%, H_2O = 8%, N_2 = balance, GHSV = 15,000 h^{-1}, catalyst weight = 1.60 g, catalyst volume = 2 ml.

the SCR activity was independent of the concentration of SO_2 in the reactant stream.

As suggested from the results of sulfation of alumina and titania (*25, 26*) sulfation not only increased Lewis acidity, but also increased Brønsted acidity when the sulfated catalysts were not completely dehydroxylated. The existence of Brønsted acid sites was shown by IR spectra of pyridine chemisorption on SO_4^{-2}/ZrO_2 and SO_4^{-2}/TiO_2 superacids. By addition of water vapor into these catalysts, a considerable amount of Lewis acid were converted to Brønsted acid sites (*12*). Isotope exchange of $^{18}O_2$ and $H_2^{18}O$ and FT-IR (*25*) results also suggest that hydroxylation of the surface sulfated titania lead to the formation of surface

TABLE 5

First-Order Rate Constants (k in $cm^3/g/s$) vs Reaction Time

Time after SO_2 injection (min.)	SO_2 concentration (ppm)						Ratio of k		
	250		500		1,000		k_3/k_1	k_3/k_2	k_2/k_1
	% Conv.	k_1	% Conv.	k_2	% Conv.	k_3			
20	37.2	2.42	48.0	3.41	85.5	10.06	4.16	2.95	1.41
25	44.5	3.07	61.5	4.97	91.6	12.90	4.21	2.59	1.62
30	52.5	3.88	73.5	6.92	94.0	14.65	3.78	2.11	1.78

Note. Reaction conditions: NO = NH_3 = 1000 ppm, O_2 = 2%, H_2O = 8% N_2 = balance, 400°C, GHSV = 15,000 h^{-1}, catalyst weight = 1.60 g, catalyst volume = 2 ml, reactant gas flow rate = 500 ml/min.

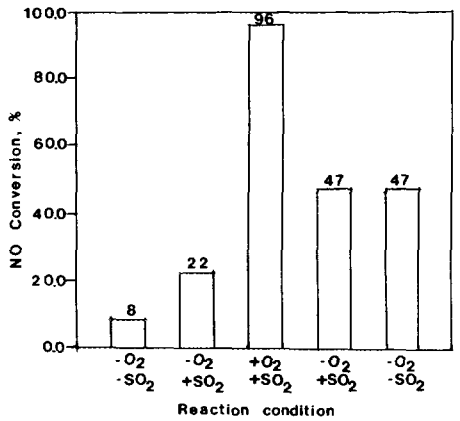

FIG. 3. NO conversion on TiO_2 under different reaction conditions. T = 400°C, NO = NH_3 = 1000 ppm, O_2 = 2% (when used), SO_2 = 500 ppm (when used), H_2O = 8%, GHSV = 15,000 h^{-1}. "+" denotes reaction with the reactant; "−" denotes reaction without the reactant.

S–OH groups. (These surface groups were apparently responsible for the SCR activity shown in Fig. 2.)

Oxygen is a necessary reactant for the sulfation when SO_2 or H_2S is used as sulfur source. Adsorption of SO_2 or H_2S on Fe_2O_3 at 400°C does not generate superacidity, but it exhibits strong acidity when oxidized with O_2 at 500°C (*22*). Figure 3 shows the effects of oxygen and sulfur dioxide on SCR titania. With no SO_2 and O_2, only 8% of NO was converted; with 500 ppm SO_2, NO conversion was increased to 22%. When both O_2 (2%) and SO_2 (500 ppm) were injected into the reactant, NO conversion reached 96%. The considerable effects of oxygen in SCR activity have been discussed extensively in the literature (*27–31*). It is interesting to note that after sulfation, even when O_2 or both O_2 and SO_2 were switched off, NO conversion still remained at 47% in contrast to 8% before sulfation. These results indicate that oxygen played an important role not only in the SCR reaction, but also in the sulfation of TiO_2.

The SO_4^{-2}/TiO_2 catalyst was also subjected to two series of stability test under the following reaction conditions: NO = NH_3 = 1000 ppm, O_2 = 2%, SO_2 = 250 ppm, H_2O = 8% (when used), 400°C and GHSV = 15,000 h^{-1}. The NO conversion maintained at 96% after 160 hrs on-stream time showing no sign of decay in activity. In the other series of test, H_2O was intermittenly admitted into the reactant during a 140-h run. The NO conversion was reversibly cycled between 96% (with water) and 98% (without water).

Characterization of Catalyst

BET surface area and TGA characterization. The BET surface area of the sulfated TiO_2 was 30 m^2/g. The TGA thermal decomposition results are shown in Fig. 4, for both TiO_2 and sulfated TiO_2. The small, continual weight loss for TiO_2 is attributed to the loss of water and hydroxyl groups from its surface. The sulfated TiO_2 underwent a two-stage weight loss: the initial one commencing at 420°C and the major one between 630 to 750°C. The weight loss was completed at near 750°C. Saur *et al.* (*25*) reported results from a similar experiment where a sulfated TiO_2 was subjected to TGA thermal decomposition *in vacuo*. Their results showed that the sulfated TiO_2 was stable up to 500°C, and that the majority of the sulfate was decomposed in the temperature range 650–720°C with no further loss above 750°C.

From the TGA results (7.28 mg SO_3/g TiO_2) and the BET surface area (30 m^2/g), the amount of SO_4^{-2} ions on the sulfated TiO_2 catalyst corresponded to 55 $Å^2$ per SO_4^{-2}.

XPS characterization. XPS spectra were measured for both unsulfated and sulfated TiO_2, shown in Figs. 5–7. The binding energies for Ti($2p_{1/2}$) and Ti($2p_{3/2}$) were the same for the unsulfated and sulfated samples, and were at 464.3 and 458.6 eV, respectively, as shown in Fig. 5, with a difference of 5.7 eV. These values are consistent with values reported in the literature (*12, 32, 33*).

Figure 6 shows the S($2p$) core-level spectra of the unsulfated and sulfated samples. The sulfated sample exhibited a peak at

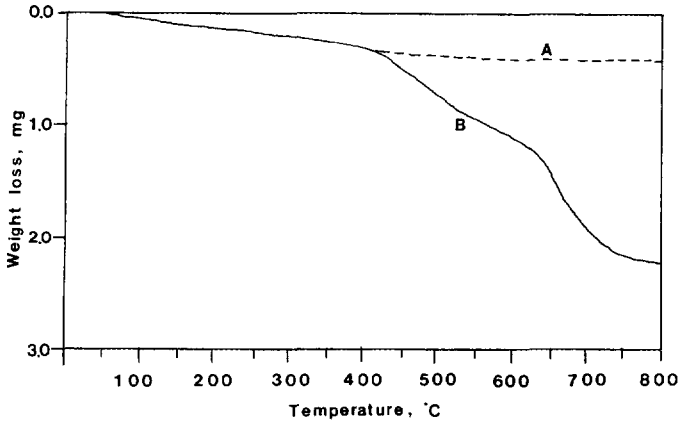

FIG. 4. TGA analysis of TiO_2 (A) and SO_4^{-2}/TiO_2 (B). Sample weight = 250 mg, heating rate = 2°C/min., in N_2 flow, N_2 flow rate = 15 ml/min.

168.5 eV. This value is typical of S^{+6} such as sulfur in Na_2SO_4, Fe_2SO_4 and $Fe_2(SO_4)_3$ (*33*).

Figure 7 shows the O(1*s*) core-level spectra. The common main peaks for the unsulfated and sulfated samples were the same, at 529.6 eV, which belonged to oxide oxygen (*12, 33, 34*). For the sulfated sample, there was an additional shoulder peak at 532 eV. This peak was attributed to sulfate oxygen (*12, 33*).

The XPS results lead to the conclusion that the surface species on the sulfated TiO_2 sample was SO_4^{-2}.

FT-IR characterization. The IR spectrum for the sulfated TiO_2 sample is shown in Fig. 8. The spectrum shows four main bands at 1382.9, 1219.1, 1124.6, and 1022.9 cm^{-1}. These are similar to but with noticeable differences from those reported by Saur *et al.* (*25*). Differences were in relative intensities and small shifts in peak positions. The weak

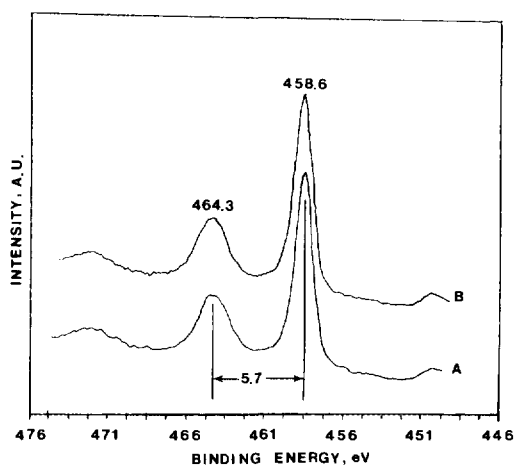

FIG. 5. XPS spectra of Ti (2*p*). (A) TiO_2; (B) SO_4^{-2}/TiO_2.

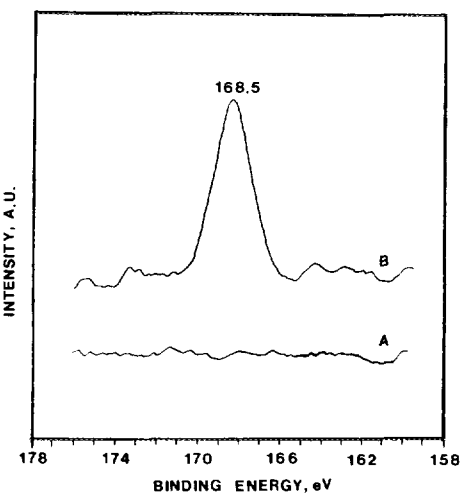

FIG. 6. XPS spectra of S (2*p*). (A) TiO_2; (B) SO_4^{-2}/TiO_2.

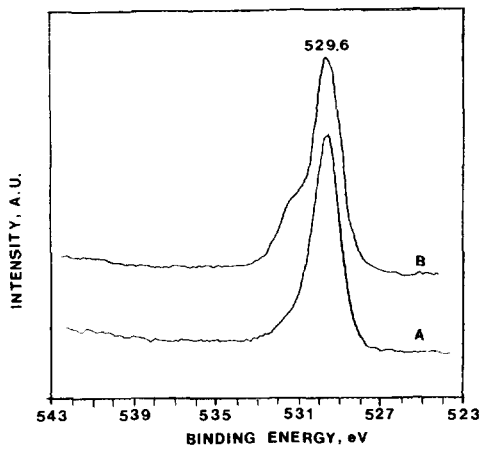

FIG. 7. XPS spectra of O (1*p*). (A) TiO_2; (B) SO_4^{-2}/TiO_2.

shoulder at 1401 cm^{-1} was assigned to NH_3 chemisorbed on Brønsted-acid sites, which was caused by the fact that the sample was subjected to SCR reaction (followed by N_2 purge at room temperature).

Infrared spectra of sulfated metal oxides generally show a strong absorption band at 1390–1375 cm^{-1} and broad bands at 1250–900 cm^{-1}. The 1390–1375 cm^{-1} peak is stretching frequency of S=O and the 1250–900 cm^{-1} peaks are the characteristic frequencies of SO_4^{-2}. The broad bands at 1250–900 cm^{-1} result from lowering of the symmetry in the free SO_4^{-2} (*Td* point group). The number and the position of the splitting peaks yield information on the symmetry of the sulfate ion and its possible configuraton.

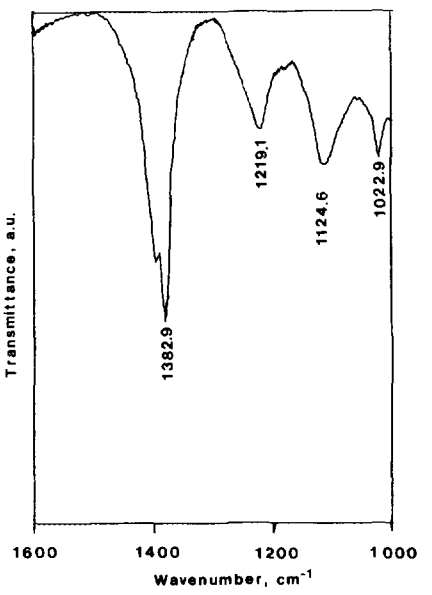

FIG. 8. IR spectrum of the sulfated titania.

The possible configurations of the sulfate ion on titania surface along with their symmetry groups are shown in Fig. 9. There are four peaks in the region 1200–400 cm^{-1} (ν_1, ν_2, ν_3, ν_4), and only ν_3 and ν_4 are infrared-active when SO_4^{-2} is a free ion (*Td* symmetry) (*35*). The value of ν_3 is 1104 cm^{-1} and ν_4 is 613 cm^{-1}. When SO_4^{-2} is bound to the titania surface, the symmetry can be lowered to either C_{3v} or C_{2v}. For C_{3v} symmetry, ν_3 split into two peaks and for C_{2v} symmetry, ν_3 split into three peaks (*35*).

As shown in Fig. 8, there are three peaks in the ν_3 region, with their peak positions matching to the literature data (*11*). Therefore, the symmetry of the sulfate ions on the TiO_2 surface should be C_{2v}. Its configuration could be either chelating bidentate or bridged bidentate, shown in Fig. 9.

The isotope exchange and IR results of Saur *et al.* (*25*) suggested that under dry conditions (no water vapor), the structure of the sulfate oxide is $(M-O)_3$ S=O, whereas under wet conditions (with water vapor), the surface structure is the bridged bidentate form with H forming a Brønsted site, $(M_2SO_4)H$.

Therefore, from the symmetry analysis of the IR spectra, the reaction conditions (with water vapor), and the isotope exchange IR spectra of Saur *et al.* (*25*), it is concluded that the sulfated titania is bridged bidentate, $Ti_2SO_3(OH)$.

Chemisorption of NO and NH_3 and Mechanistic Implications

The SCR reaction mechanism has been open to debate since 1970s, mostly on the V_2O_5/TiO_2 catalyst. Both Langmuir–Hinshelwood (*36–38, 42, 43*) and Eley–Rideal

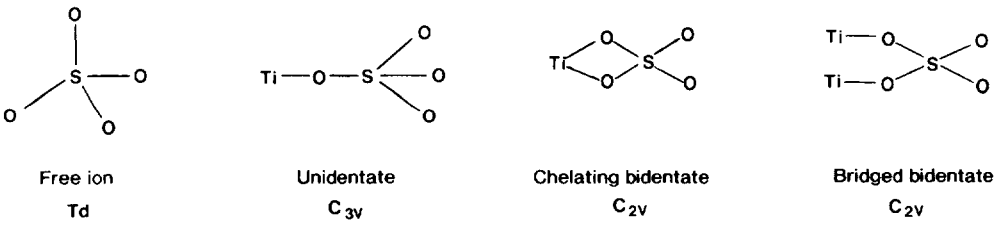

FIG. 9. The structure of free SO_4^{-2} and its possible configurations on the titania surface.

(*3, 27, 44–48*) mechanisms have been proposed. In the Langmuir–Hinshelwood mechanism, the oxidation–reduction scheme has been proposed for the V_2O_5/TiO_2 catalyst, where the catalyst is reduced by NH_3 and re-oxidized by NO or O_2. This mechanism may be valid for oxide catalysts that are reducible under the SCR conditions. Since SO_4^{-2}/TiO_2 is hardly reducible by NH_3 under the SCR conditions, the redox mechanism is not plausible.

To understand the reaction mechanism, the amounts of NH_3 and NO chemisorbed at 400°C were measured, for both TiO_2 and SO_4^{-2}/TiO_2 samples. The same flow reactor system was used for this measurement. The influent concentration (of NH_3 or NO, separately) was constant at 1000 ppm while the effluent concentration was continually measured. The difference yielded the chemisorbed amount. More details of the technique were given elsewhere (*3*). The results are listed in Table 6.

The results showed that, at 400°C, TiO_2 chemisorbed a large amount of NH_3, but no NO. The SO_4^{-2}/TiO_2 chemisorbed significantly more NH_3 (about 47% more) than TiO_2. This suggests that sulfation of TiO_2 created new acid sites. Moreover, a small amount of NO was also chemisorbed on SO_4^{-2}/TiO_2. The population densities of NH_3 and NO are also given in Table 6. The chemisorbed NH_3 was densely populated on both TiO_2 and SO_4^{-2}/TiO_2 surfaces, corresponding to 0.7 NH_3 per surface SO_4^{-2} ion on SO_4^{-2}/TiO_2.

TABLE 6

Chemisorption Amounts of NH_3 and NO

Catalyst	Chemisorbed amount			
	NH_3		NO	
	cc STP/g	molecule/nm^2	cc STP/g	molecule/nm^2
TiO_2	0.929	0.83	0	0
SO_4^{-2}/TiO_2	1.372	1.23	0.024	0.022

Note. Conditions: T = 400°C, NO = NH_3 = 1000 ppm (used separately), O_2 = 2%, N_2 = balance, flowrate = 500 cc/min, catalyst = 1.0 g.

Following the measurements of the chemisorbed NH_3 and NO on the SO_4^{-2}/TiO_2 catalyst, a further experiment was undertaken to elucidate the mechanism. The catalyst was first saturated with NH_3 chemisorption (under the same conditions listed in Table 6, but without NO). The influent was then switched to a flow containing 1000 ppm NO and 2% O_2 (in N_2), and the NO conversion was continually recorded. The NO conversion was over 90% during the first minute, decreased to zero in about 4 min, when the active chemisorbed NH_3 was consumed. The data indicated that about 52% of the chemisorbed NH_3 was active, and was consumed by NO for conversion. The remaining 48% of the chemisorbed NH_3 was inactive or desorbed during the reaction.

To provide further insights into the reaction mechanism, XPS was used to analyze the surface structures of the catalysts. Two catalyst samples, TiO_2 and SO_4^{-2}/TiO_2, were subjected to SCR reaction at 400°C for 150 h. The catalysts were cooled to room temperature in the reaction atmosphere, followed by purge in N_2 for 1 h. The samples

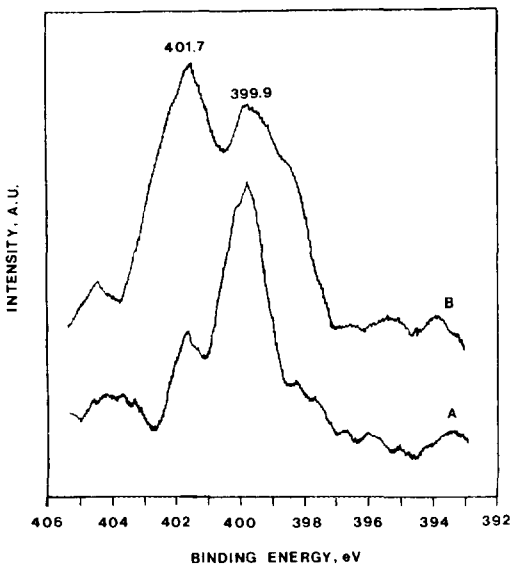

FIG. 10. XPS spectra of N (1*s*). (A) TiO_2; (B) SO_4^{-2}/TiO_2.

were then subjected to XPS analysis. The XPS spectra for the two samples are shown in Fig. 10.

Two peaks are seen in the XPS spectra, 399.9 and 401.7 eV. The major difference between the spectra of the two samples was that the peak at 401.7 eV was considerably enhanced for the SO_4^{-2}/TiO_2 sample over that for the TiO_2 sample.

The possible interpretation for the XPS result is that the N(1*s*) peaks in Fig. 10 belong to the chemisorbed NH_3. The peak at 399.9 eV can be assigned to ammonia chemisorbed on the Lewis acid sites on TiO_2 or SO_4^{-2}/TiO_2. The binding energy of 399.9 eV is 1 eV higher than that of free NH_3 (a Lewis base) of 398.9 eV (*39*). Electron donation from the lone pair electrons of NH_3 to the Lewis-acid site leads to a higher binding energy than that of free NH_3.

The peak at 401.7 eV in Fig. 10 can be assigned to ammonia chemisorbed on Brønsted-acid sites, because its value is the same as or close to the values reported in the literature. The binding energies of N(1*s*) in NH_4Cl (*40*) and NH_4NO_3 (*41*) are 401.7 and 401.9 eV, respectively. The chemisorption of ammonia on Brønsted acid sites is in the form of NH_4^+, which could attach to the surface sulfate ion.

Along with results on the SCR activity and the NH_3 and NO chemisorption measurements, this assignment would indicate that SCR activity of the SO_4^{-2}/TiO_2 catalyst is directly related to the XPS peak at 401.7 eV, i.e., NH_3 chemisorbed on its Brønsted-acid sites. It may be concluded that active sites for SCR reaction on this catalyst are Brønsted-acid sites and that the reaction mechanism follows an Eley–Rideal type.

ACKNOWLEDGMENTS

This work was supported by Electric Power Research Institute. Helpful discussions with J. E. Cichanowicz of EPRI are acknowledged.

REFERENCES

1. Bosch, H., and Janssen, F., *Catal. Today* **2**, 369 (1988).
2. Chen, J. P., and Yang, R. T., *Appl. Catal.* **80**, 135 (1992).
3. Chen, J. P., and Yang, R. T., *J. Catal.* **125**, 411 (1990).
4. Chen, J. P., Yang, R. T., Buzanowski, M. A., and Cichanowicz, J. E., *Ind. Eng. Chem. Res.* **29**, 1431 (1990).
5. Hino, M., and Arata, K., *J. Chem. Soc., Chem. Commun.*, 1148 (1979).
6. Hino, M., Kobayasi, S., and Arata, K., *J. Am. Chem. Soc.* **1**, 6439 (1979).
7. Hino, M., and Arata, K., *J. Chem. Soc., Chem. Commun.*, 851 (1980).
8. Gillespie, R. J., *Acc. Chem. Res.* **1**, 202 (1968).
9. Gillespie, R. J., and Pell, T. E., *Adv. Phys. Org. Chem.* **9**, 1 (1972).
10. Tanabe, K., Misono, M., Ono, Y., and Hattorio, H., "New Solid Acids and Bases, Their Catalytic Properties," p. 199. Kodansha, Tokyo, 1989.
11. Yamaguichi, T., *Appl. Catal.* **61**, 1 (1990).
12. Arata, K., *in* "Advances in Catalysis" (D. D. Eley, H. Pines, and P. B. Weise, Eds.). Vol. 37, p. 165. Academic Press, San Diego, 1990.
13. Olah, G. A., Prakash, G. K. S., and Sommer, J., "Supracids." Wiley, New York, 1985.
14. Bond, G. C., Zurita, J. P., and Flammerz, S., *Appl. Catal.* **27**, 353 (1986).
15. Kang, Z. C., and Bao, Q. X., *Appl. Catal.* **26**, 251 (1986).
16. Saleh, R. Y., Wachs, I. E., Chan, S. S., and Cwersich, C. C., *J. Catal.* **98**, 102 (1986).
17. Baiker, A., Dollenmeier, P., and Glinski, M., *Appl. Catal.* **35**, 351 (1987).

18. Kataoka, T., and Dumesic, J. A., *J. Catal.* **112,** 66, (1988).
19. Tanabe, K., Ishiya, C., Matsuzaki, I., Ichikawa, I., and Harttori, H., *Bull. Chem. Soc. Jpn.* **45,** 47 (1972).
20. Kung, M. C., and Kung, H. H., *Catal. Rev.-Sci. Eng.* **27,** 425 (1985).
21. Tanabe, K., Misono, M., Ono, Y., and Hattori, H., "New Solid Acids and Bases. Their Catalytic Properties," p. 48. Kodansha, Tokyo, 1989.
22. Yamaguchi, T., Jin, T., and Tanabe, K., *J. Phys. Chem.* **90,** 3148 (1986).
23. Tanabe, K., *in* "Heterogeneous Catalysis" (B. L. Shapiro, Ed.), p. 71. Texas A & M Univ., College Station, TX, 1984.
24. Yamaguchi, T., and Tanabe, K., *Mater. Chem. Phys.* **16,** 67 (1986).
25. Saur, O., Bensitel, M., Mohammed Saad, A. B., Lavalley, J. C. Tripp, C. P., and Morrow, B. A., *J. Catal.* **99,** 104 (1986).
26. Busca, G., Saussey, H., Saur, O., Lavalley, J. C., and Lorenzelli, V., *Appl. Catal.* **14,** 245 (1985).
27. Inomata, M., Miyamoto, A., and Murakami, Y., *J. Catal.* **62,** 150 (1980).
28. Bauerle, G. L., Wu, S. C., and Nobe, K., *Ind. Eng. Chem. Prod. Res. Dev.* **14,** 268 (1975).
29. Shikada, T., Fujimoto, K., Kung, T., Tominaga, H., Kaneko, S., and Kubo, Y., *Ind. Eng. Chem. Prod. Res. Dev.* **20,** 91 (1981).
30. Bosch, H., Janssen, F. J. J. G., Oldenziel, J., van den Kerkhof, F. M. G., van Ommen, J. G., and Ross, J. R. H., *Appl. Catal.* **25,** 239 (1986).
31. Wong, W. C., and Nobe, K., *Ind. Eng. Chem. Prod. Res. Dev.* **25,** 179 (1986).
32. Hendrickson, C. D., Hollander, J. M., and Jolly, W., *Inorg. Chem.* **8,** 2642 (1969).
33. Wagner C. D., Riggs, W. M., Davis, L. E., and Moulder, J. F., *in* "Handbook of X-ray Photoelectron Spectroscopy" (G. E. Muilenberg, Ed.), Perkin–Elmer Corp., U.S.A., 1979.
34. Wagner, C. D., *in* "Practical Surface Analysis" (D. Briggs and M. D. Seah, Eds.), 2nd Ed., p. 599. Wiley, Chichester, UK, 1990.
35. Nakamoto, K., "Infrared and Raman Spectra of Inorganic and Coordination Compounds," 4th ed. Wiley, New York, 1986.
36. Odriozola, J. A., Heinemann, H., Somorjai, G. A., Garecia de la Banda, J. F., and Pereira, P., *J. Catal.* **119,** 71 (1989).
37. Odriozola, J. A., Soria, J., Somorjai, G. A., Heinemann, H., Garcia de la Banda, J. F., Granados, M. L., and Conesa, J. C., *J. Phys. Chem.* **95,** 240 (1991).
38. Takagi, M., Kawai, T., Soma, M., Onishi, T., and Tamaru, K., *J. Catal.* **50,** 441 (1977).
39. Larkins, F. P., and Lubenfeld, A., *J. Electron Spectrosc. Relat. Phenom.* **15,** 137 (1979).
40. Burger, K., Tschismarov, F., and Ebel, H., *J. Electron Spectrosc. Relat. Phenom.* **10,** 461 (1977).
41. Barbaray, B., Contour, J. P., and Mouvier, G., *Environ. Sci. Technol.* **12,** 1294 (1978).
42. Takagi, M., Kawai, T., Soma, M., Onishi, T., and Tamaru, K., *J. Phys. Chem.* **80,** 430 (1976).
43. Takagi, M., Kawai, T., Soma, M., Onishi, T., and Tamaru, K., *Can. J. Chem.* **58,** 2132 (1980).
44. Miyamoto, A., Inomata, M., Yamazaki, Y., and Murakami, Y., *J. Catal.* **57,** 526 (1979).
45. Miyamoto, A., Kobayashi, K., Inomata, M., and Murakami, Y., *J. Phys. Chem.* **86,** 2945 (1982).
46. Wu, S. C., and Nobe, K., *Ind. Eng. Chem. Prod. Res. Dev.* **16,** 136 (1977).
47. Miyamoto, A., Yamazaki, Y., Hattori, T., Inomata, M., and Murakami, Y., *J. Catal.* **74,** 144 (1982).
48. Otto, K., Shelef, M., and Kummer, J. T., *J. Phys. Chem.* **74,** 2690 (1970).
49. Kokkinos, A., Cichanowicz, J. E., Hall, R. E., and Sedman, C. B., *J. Air Waste Manage. Assoc.* **41,** 1252 (1992), and literature cited therein.
50. Sohn, J. R., and Jang, H. J., *J. Catal.* **136,** 267 (1992).
51. Chen, J. P., Buzanowski, M. A., Yang, R. T., and Cichanowicz, J. E., *J. Air Waste Manage. Assoc.* **40,** 1403 (1990).
52. Yang, R. T., Chen, J. P., Kikkinides, E. S., Cheng, L. S., and Cichanowicz, J. E., *Ind. Eng. Chem. Res.* **31,** 1440 (1992).
53. Nam, I., Eldridge, J. W., and Kittrell, J. R., *Ind. Eng. Chem. Prod. Res. Dev.* **25,** 186 (1986).
54. Nam, I., Eldridge, J. W., Kittrell, J. R., *in* "Catalysis 1987" (J. W. Ward, Ed.), p. 589. Elsevier, Amsterdam, 1988.
55. van Tol, M. F. H., Quinlan, M. A., Luck, F., Somorjai, G. A., and Nieuwenhuys, B. E., *J. Catal.* **129,** 186 (1991).
56. Naruse, Y., Ogasawara, T., Hata, T., and Kishitaka, H., *Ind. Eng. Chem. Prod. Res. Dev.* **19,** 57 (1980).